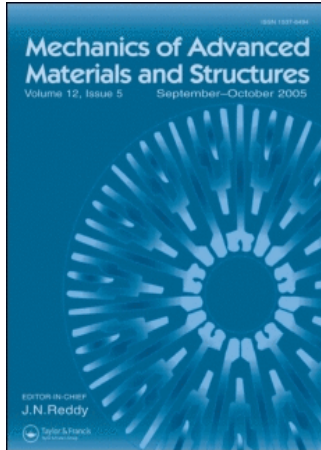


This article was downloaded by:[HEAL-Link Consortium]  
On: 22 February 2008  
Access Details: [subscription number 786636650]  
Publisher: Taylor & Francis  
Informa Ltd Registered in England and Wales Registered Number: 1072954  
Registered office: Mortimer House, 37-41 Mortimer Street, London W1T 3JH, UK



## Mechanics of Advanced Materials and Structures

Publication details, including instructions for authors and subscription information:  
<http://www.informaworld.com/smpp/title~content=t713773278>

### FREE EDGE EFFECT ON RESIDUAL STRESSES AND DEBOND OF A COMPOSITE FIBRE/MATRIX INTERFACE

Shoufeng Hu <sup>a</sup>; Prasanna Karpur <sup>b</sup>; Theodore E. Matikas <sup>b</sup>; Leon Shaw <sup>c</sup>; Nicholas J. Pagano <sup>d</sup>

<sup>a</sup> WL/MLLP, Materials Directorate, Wright Laboratory, OH, USA

<sup>b</sup> Research Institute, University of Dayton, Dayton, OH, USA

<sup>c</sup> Systran Corporation, Dayton, OH, U.S.A

<sup>d</sup> Materials Directorate, Wright Laboratory, OH, USA

Online Publication Date: 01 September 1995

To cite this Article: Hu, Shoufeng, Karpur, Prasanna, Matikas, Theodore E., Shaw, Leon and Pagano, Nicholas J. (1995) 'FREE EDGE EFFECT ON RESIDUAL STRESSES AND DEBOND OF A COMPOSITE FIBRE/MATRIX INTERFACE', *Mechanics of Advanced Materials and Structures*, 2:3, 215 - 225

To link to this article: DOI: 10.1080/10759419508945841

URL: <http://dx.doi.org/10.1080/10759419508945841>

PLEASE SCROLL DOWN FOR ARTICLE

Full terms and conditions of use: <http://www.informaworld.com/terms-and-conditions-of-access.pdf>

This article maybe used for research, teaching and private study purposes. Any substantial or systematic reproduction, re-distribution, re-selling, loan or sub-licensing, systematic supply or distribution in any form to anyone is expressly forbidden.

The publisher does not give any warranty express or implied or make any representation that the contents will be complete or accurate or up to date. The accuracy of any instructions, formulae and drug doses should be independently verified with primary sources. The publisher shall not be liable for any loss, actions, claims, proceedings, demand or costs or damages whatsoever or howsoever caused arising directly or indirectly in connection with or arising out of the use of this material.

# FREE EDGE EFFECT ON RESIDUAL STRESSES AND DEBOND OF A COMPOSITE FIBRE / MATRIX INTERFACE

SHOUFENG HU

*WL / MLLP, Materials Directorate, Wright Laboratory, Wright-Patterson AFB, OH 45433, U.S.A.*

PRASANNA KARPUR AND THEODORE E. MATIKAS

*Research Institute, University of Dayton, Dayton, OH 45469, U.S.A.*

LEON SHAW

*Systran Corporation, Dayton, OH 45432, U.S.A.*

NICHOLAS J. PAGANO

*Materials Directorate, Wright Laboratory, Wright-Patterson AFB, OH 45433, U.S.A.*

## SUMMARY

In this study, the free edge effect on the fibre matrix interface of a single fibre metal matrix composite has been investigated. It was found, using both an approximate elasticity model and finite element analysis, that the interfacial radial residual stress has a reversal in sign, from negative to positive with a high gradient, in the neighbourhood of a free edge. An additional finite element analysis, using contact element at the interface, predicted that the stress reversal would produce a sizeable circumferential interfacial debond, assuming zero interfacial tensile strength. Finally, an ultrasonic non-destructive evaluation technique has indirectly illustrated the existence of this interfacial debond prior to any mechanical loading. The method of phase alteration of back-reflected ultrasonic shear wave has provided a new approach for detecting microscopic scale failure in composites.

## INTRODUCTION

The problem of edge effect was initially introduced for interlaminar stresses in laminated composites at free edges by Pipes and Pagano<sup>1</sup>, and it has been studied extensively. The classical lamination theory describes the laminated composite behaviour using an assumption of a generalized plane stress state. This assumption turns out to be quite valid in the interior of the laminate, assuming that no internal stress riser, such as holes or cracks, exists. However, in the neighbourhood of a free edge extending a distance approximately equal to the laminate thickness, there exists a complex three-dimensional stress state. This free edge effect leads to an elastic stress singularity at a perfectly bonded interface of a laminate under mechanical or thermal loading.

On the microscopic scale a fibre and the surrounding matrix suffer a similar stress complexity in the neighbourhood of a free edge where the fibre ends are exposed. Recently, Pagano<sup>2,3</sup> developed an approximate elasticity model to study the response of an axisymmetric, multi-concentric cylinder, multi-material composite system. The model, using an assumption of linear hoop and axial stresses in the radial direction within each concentric cylinder, satisfies all equilibrium equations, interface continuity conditions and other applicable boundary conditions. The use of Reissner's variational theorem<sup>4</sup> provides the appropriate governing field equations. In addition, several concentric cylinders can be used in one material (e.g., matrix) to further minimize the error introduced by the assumption of some of the stress components. Although the model presents no singularity at the free edge due to the solution technique employed, excellent agreement with other approximate elasticity models has been achieved<sup>2,3</sup>.

In this model, Pagano predicted the sign reversal of radial stress in the stress singular region. For composites of titanium matrix reinforced with silicon carbide fibres, the matrix coefficient of thermal expansion (CTE) is much larger than fibre CTE, resulting in a large and negative thermally induced residual stress at the fibre/matrix interface away from the ends. Nonetheless, the model predicts that in the neighbourhood of the free edge within a fibre radius there exists a very steep gradient in radial stress varying from negative to positive. Whether the weak metal matrix composites (MMCs) fibre/matrix interface responds to such a highly localized stress distribution, however, needs to be studied by experiment. For this work, we shall undertake such a study. In figure 1, the mechanism of the stress singularity is illustrated along with the consequent interface fracture due to the mismatch of CTEs in fibre longitudinal direction.

In this study we investigated the free edge effect on the redistribution of residual stresses and debonding behaviour at the interface of a titanium matrix cylinder reinforced with a single silicon carbide fibre. The aim of the present study is to display the existence of radial stress reversal, the high stress gradient due to the stress singularity, and the interface debond created by the radial tensile stress singularity. To achieve this, we used theoretical modelling (Pagano's model), numerical analysis (finite element stress analysis) and experimental investigation (non-destructive ultrasonic evaluation technique).

The results presented in this study were obtained from the samples of single fibre composite. However, they can be applied to unidirectional composites<sup>5,6</sup>. There are several reasons for using a single fibre composite as a test specimen. First, in a single fibre composite we focus on one specific fibre. If we are only interested in local damage such as interfacial debonding, a single fibre composite avoids the distraction of randomness in failure and the neighbouring effect of other fibres in unidirectional composites. Next, manufacturing the sample of a single fibre composite is much more cost-effective and easier than the unidirectional composites for MMCs. At early stage of research, a single fibre composite reveals much of the information needed for composite characterization. Without using the single fibre composite samples, some research would be prohibitive because of the cost of unidirectional MMCs. Therefore, although a single fibre composite is not exactly equivalent to the real-world



Figure 1. Exaggerated schematic view of the interfacial crack due to the free edge effect in a single fibre composite after being processed

composites, we believe that the role played by the single fibre composite for MMC research may not be replaced in the foreseeable future.

### MATERIALS

The samples used for experiment are titanium aluminide matrix Ti-6Al-4V reinforced with a single silicon carbide Textron SCS-6 fibre. The fibre is aligned by placing it in a fibre retention groove in a titanium preform plate that was machined with a specially constructed shaping apparatus. Samples were fabricated by hot pressing at a condition of 900° C at 17 MPa for 1.5 hours. The room temperature thermomechanical properties for fibre and matrix are given in Table I.

The samples were originally designed for a single fibre composite transverse test, as illustrated in Figure 2. However, the free edge effect is studied when the sample was under no applied stress. The fibre volume fraction in a single fibre composite sample approaches zero and the free edge disturbance occurs in a region less than two fibre diameters in length. We therefore believe that in terms of the free edge effect, the sample is equivalent to a fibre aligned along the  $z$ -axis embedded in an infinite half space of matrix above the plane  $z = 0$ . A parametric study suggested that if the diameter of the matrix cylinder is five times the fibre diameter, which is used in the analytical and numerical studies, or larger, the geometric effect on the magnitudes and distributions of residual stresses is negligible.

The sample dimensions are 5.54 mm in width, 2.33 mm in thickness, and 65 mm in gauge length.

Some studies (e.g. Reference 7) suggest that for MMCs of titanium matrix reinforced with silicon carbide fibres interfacial contact is primarily due to thermal clamping stress in the radial direction. Chemical diffusion and reaction bonds, if any, are considered weak. In order to understand the interfacial bond strength, we need to consider the structure of the 'interphase' between fibre and matrix. Prior to processing, an SCS-6 fibre has a 2–4  $\mu\text{m}$  thick carbon coating which is deposited in the latest stage of chemical vapour deposition during production. After the sample is hot-pressed, this coating remains, although a small part of it reacts with the adjacent matrix. This carbonaceous layer of SCS-6 fibre consists of the so-called turbostratic carbon blocks. The bonding between the basal planes of turbostratic carbon blocks is of the weak van der Waals type<sup>8</sup>. This supports the claim that the tensile strength of the interfacial bond is almost zero.

### STRESS ANALYSIS

A typical model of micromechanical stress analysis for a single fibre composite is that of a circular cylindrical body of one material (fibre) surrounded by one or several concentric annuli

Table I. Room temperature thermomechanical properties for fibre and matrix

|           | Young's<br>modulus (GPa) | Shear<br>modulus (GPa) | Poisson's<br>ratio | CTE<br>( $\times 10^{-6}/^{\circ}\text{C}$ ) |
|-----------|--------------------------|------------------------|--------------------|--|
| Ti-6Al-4V | 118.8                    | 45.0                   | 0.32               | 9.0  |
| SCS-6     | 410.7                    |                        | 0.15               | 3.99   |

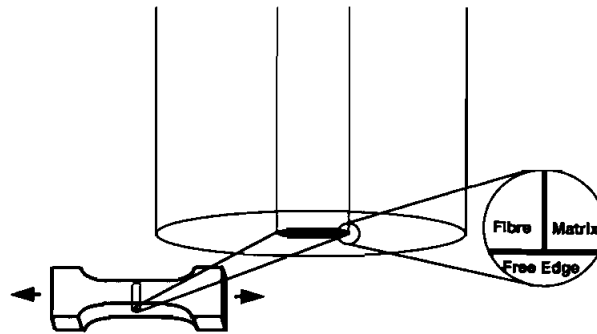


Figure 2. The configuration for analysis

of other materials (interphase or matrix). Since very limited information on the interphase is available, we do not include it in the analysis. Since the interphase is so thin, it serves primarily as a bonding/debonding agent between fibre and matrix, i.e. it has negligible effect on the fibre and matrix stresses. This was demonstrated by executing a parametric study to determine the effect of interphase stiffness on the latter stresses.

A two-dimensional axisymmetric finite element analysis for this problem has been performed. The configuration and the related boundary conditions used in the analysis are shown in Figures 2 and 4. The diameter ratio of outer cylinder (matrix) to inner cylinder (fibre) is five, which provides a good simulation of a single fibre in an infinite medium. Using the commercially available finite element package ANSYS 5.0, we were able to model not only the stress state near the stress singular point but also the interfacial debonding behaviour caused by tensile radial stress. In this study we used a total of 14 000 two-dimensional linear four-noded rectangular elements. The mesh in the region of interest, which extends from the free edge approximately one fibre diameter, is very fine (one-hundredth of the fibre diameter) to capture the high stress gradients in the region.

We divided our effort of numerical analysis into three cases. In the first case, we performed the finite element analysis described above. The stresses in the neighbourhood of the singular point were used to compare with the results of Pagano's approximate elasticity model discussed earlier. Doing this allows us to examine the fidelity of the finite element analysis. The comparison shows that the agreement between the two models is excellent except the last point (see Figure 3). The free edge node discrepancies are expected, since there exists a stress singularity which has not been incorporated into either model.

The approximate elasticity model also includes the capability to characterize a sudden material elastic property change in the longitudinal direction<sup>9</sup>, which allows this model to predict the stress state in the embedded fibre problem (see Figure 4). The interior singularity at the fibre 'corner', i.e. the cross-line of two interfaces, manifests itself by producing a discontinuity in the axial distribution of the radial stress which approaches negative infinity on the interface. While there is no tendency to debond the interface, there exists a region of high tensile radial stress in the matrix at the region beyond the corner. This tensile radial residual stress can be understood by introducing an 'imaginary' interface, which extends from the fibre tip to the free edge (see Figure 4(b)). The 'imaginary' fibre (actually matrix) has a much higher CTE than the real fibre. As a result of cooling, an additional compressive radial stress at the tip of a real fibre and a tensile radial stress at the 'imaginary' fibre are created due to this mismatch of CTEs in transverse direction. We further performed a finite element analysis of

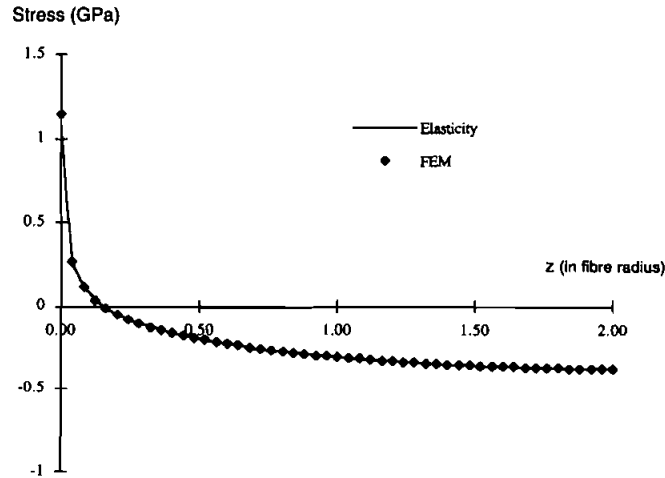


Figure 3. The edge effect on interfacial residual stress: radial stress reversal.  $z = 0$  is the free edge

the embedded fibre problem (second case). The comparison between analytical and numerical results is illustrated in Figure 5. The agreement, similar to first case, is excellent except for the node at the singular point.

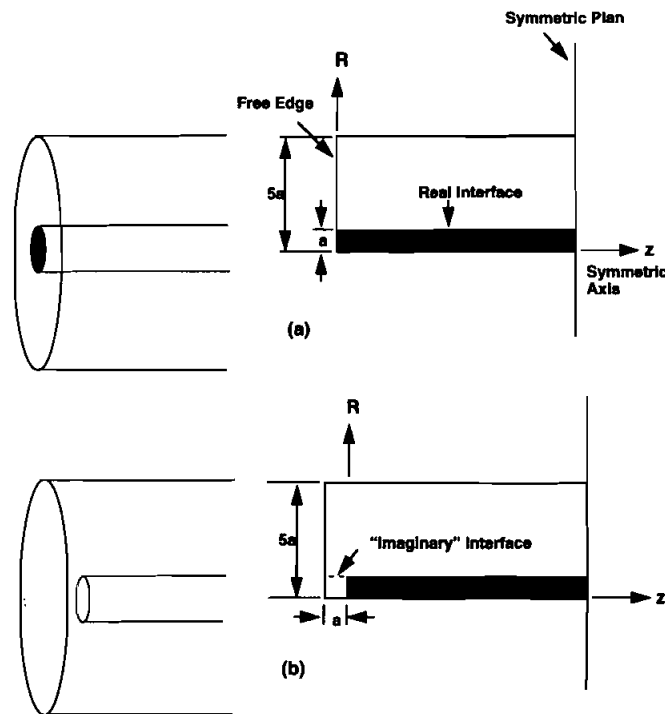


Figure 4. The schematic views, dimensions, and boundary conditions of single fibre composites (a) with the free edge and (b) with an embedded fibre.  $a$  (0.071 mm) is the radius of fibre.

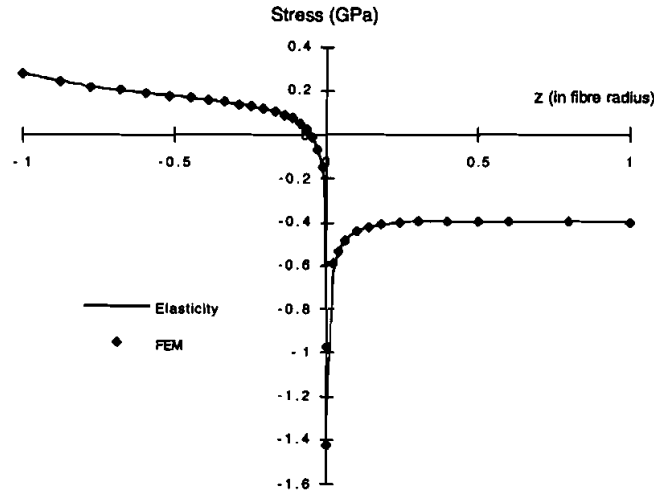


Figure 5. Radial residual stress at the interface of composite with an embedded fibre. Positive  $z$  axis is the real interface; negative  $z$  axis is the 'imaginary' interface;  $z = 0$  is the longitudinal interface; and  $z = -1$  is the free edge.

Finally, the interfacial debond is simulated using bi-linear contact elements<sup>10</sup> at the possible debonding area in third case of finite element analysis. The contact element is dimensionless prior to any loading and presents a bilinear stress/strain relationship under loading. When in tension, the element does not function, which allows for the physical separation of fibre and matrix. When in compression, the element functions like a stiff spring which permits continuity of radial stress and displacement by allowing minimum penetration of matrix into fibre. The spring constant is chosen to be an order of magnitude greater than the stiffness of the adjacent material with a higher stiffness<sup>10</sup>. A friction coefficient of 0.75 was used for possible interfacial sliding. This coefficient is experimentally measured by Waterbury<sup>11</sup> and has been found sample-dependent. We have found that the computed debond length is insensitive to the value used for coefficient of friction. Ideally, the spring constant should be infinite to prevent any unrealistic physical penetration. But in reality a large spring constant will introduce extensive numerical error in the process leading to a very slow convergence or even failure to converge. The finite element analysis of the third case predicts a circumferential interfacial debond of length  $20 \mu\text{m}$  starting from the free edge. The maximum crack opening displacement, approximately  $0.04 \mu\text{m}$ , is found at the free edge.

The first case in the finite element analyses represents an idealized problem because the interface can not support a singular tensile radial stress. For the second and third cases it is necessary to discuss the effect of plasticity. In the global finite element analyses, maximum and minimum stresses can be easily obtained. The results showed that in the third case both maximum (tensile) and minimum (compressive) von Mises yield stresses are less than the titanium yield stress (approximately 900 MPa) because of the stress relief due to the interfacial debond. However, in the second case the negative singular radial stress exists at the fibre 'corner'. In the model we have neglected the (expected) small zone of plasticity that occurs in the region of very high stress gradients.

## EXPERIMENTAL STUDY

Ultrasonic waves have a long history of use for structural non-destructive evaluation (NDE).

They have been successful in investigation of mechanical flaws, structural dimensions, and material elastic properties. In short, ultrasonic waves can be used to detect anything that affects elastic wave propagation.

Recently, a new NDE technique—ultrasonic shear wave back-reflectivity (SBR)—has been developed<sup>12</sup> for characterizing the fibre/matrix interface of metal matrix composites (MMCs) and ceramic matrix composites (CMCs). For titanium MMCs the ultrasonic wave front was incident on the matrix at an angle of  $24^\circ$  to image the embedded fibre (see Figure 6). This angle is selected for the maximum reflection of the energy in the titanium matrix material. As a result, vertically polarized shear waves are incident on the fibre/matrix interface. There are several advantages of using shear waves instead of longitudinal waves. First, shear waves have shorter wavelengths, which leads to a higher resolution. Next, shear waves are more sensitive to failure of the interfacial bond. But above all, since the wave front was incident at an angle, the received shear wave signal was either low in amplitude due to lack-scattering from the material grain structure or very strong in amplitude due to the back-reflection from the cylindrical fibre. In this study we used a 25-MHz focused ultrasonic transducer to produce ultrasonic C-scan images of the silicon carbide fibres in titanium MMCs. The focal area has an approximate diameter of  $150\ \mu\text{m}$ .

## RESULTS AND DISCUSSION

The samples were originally designed for the test of single fibre interfacial strength under transverse loading. However, it has been observed that SBR image of the fibre in a single fibre composite sample prior to any mechanical loading has two separate parts near the ends<sup>13, 14</sup> (see Figure 7(a)). This phenomenon of image separation occurs in all of the single fibre composite samples and some of the laminated composites we have scanned using ultrasonic NDE techniques. It occurs not only in MMCs but in CMCs as well. On the other hand, if the fibre is entirely embedded inside the matrix these separations disappear<sup>15</sup> (Figure 7(b)). Further, we have C-scanned a sample of titanium plate with a cylindrical hole<sup>16</sup>. The hole has the same diameter as the fibre and passes through the entire plate width. The ultrasonic image of this hole shows no separation parts either (Figure 7(c)). This eliminates the possibility that the image separation is created by ultrasonic wave interference due to the sample edge.

We claim that the primary reason for image separation is the reflected signal phase alteration<sup>13,14</sup>. There are three factors which characterize an acoustic wave propagation. They

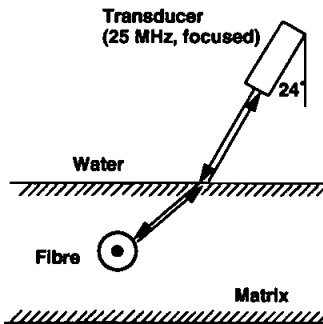


Figure 6. Schematic of the experimental set-up of ultrasonic shear wave reflection for the single fibre composite.



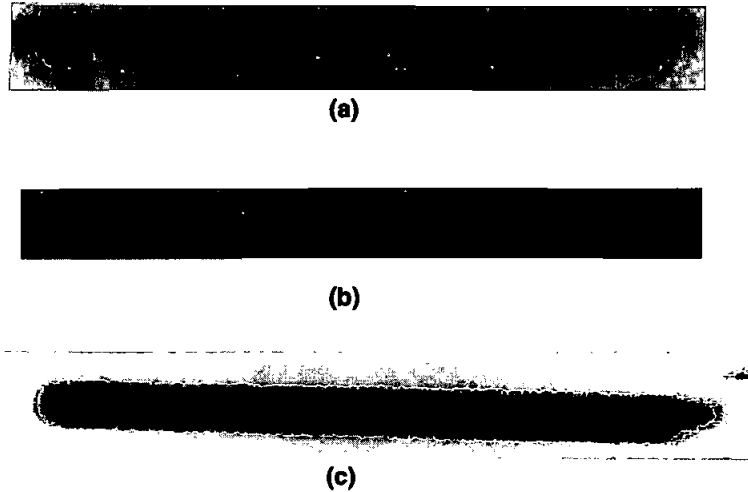


Figure 7. Ultrasonic images of (a) a single fibre with free edge, (b) an embedded single fibre, and (c) a cylindrical hole with the same size as the fibre.

are displacement amplitude, wavelength (or frequency), and phase angle. Imagine that two waves propagate from the same origin and in the same direction. If they have the same amplitude and the same wavelength but the phase angles are  $180^\circ$  apart, the superposed wave will disappear. This represents the effect of the wave (or signal) cancellation due to the phase alteration. The ultrasonic wave reflection from an interface is dependent on the material acoustic impedance. Since the ultrasonic beam is normally incident to the circumference of the cylindrical fibre and the fibre diameter is about the same as the wavelength of the incident shear wave, we assume that the back reflection can be considered as a localized one-dimensional problem. The coefficient of reflection,  $R$ , is expressed as<sup>17</sup>

$$R = \frac{Z_2 - Z_1}{Z_2 + Z_1} = \frac{\rho_2 C_2 - \rho_1 C_1}{\rho_2 C_2 + \rho_1 C_1} = \frac{\sqrt{\rho_2 G_2} - \sqrt{\rho_1 G_1}}{\sqrt{\rho_2 G_2} + \sqrt{\rho_1 G_1}}$$

where  $Z, C, \rho$  and  $G$  are the material acoustic impedance, shear wave velocity, density, and shear modulus respectively, and subscripts 1 and 2 represent the media in which the incident wave and the transmitted wave travel, respectively.

Figure 8 illustrates three different positions of the interface (A, B, and C) which the focal area of incident ultrasonic wave covers. In case A at which interface is well bonded, medium 1 (matrix) has a much smaller impedance than medium 2 (fibre). Consequently, the reflective signal is in phase; i.e., it has the same phase angle as the incident wave. In case C, the incident wave basically covers only the debonded area where the medium 2 (the material filling the gap which will be explained later) has a much lower acoustic impedance than of medium 1 (matrix). The reflection signal changes to out of phase, meaning that it has a phase angle  $180^\circ$  different from that of the incident wave. If the focal area of the ultrasonic beam covers part of debonded area with out of phase signal and part of well bonded area with in phase signal (case B), the reflective signal received by the transducer will be partially or totally cancelled out owing to this signal phase alteration.

The next question arises: if there exists a interfacial debond prior to any mechanical loading, can we reliably see it? The answer is no. We cannot see it even with the aid of

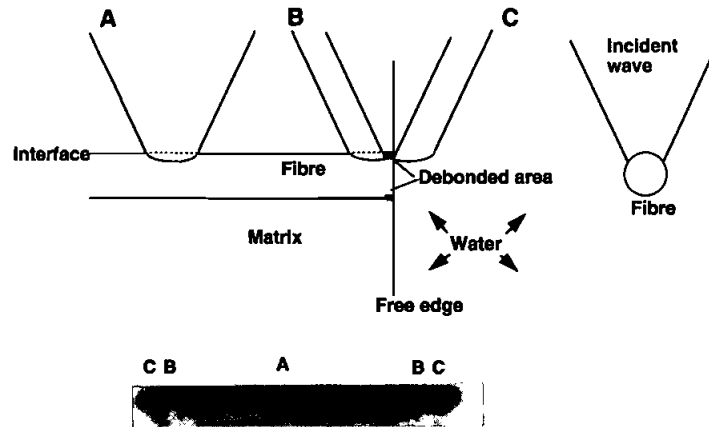


Figure 8. Incident shear wave (A) covers well-bonded interface, (B) partially covers bonded and debonded interface regions and (C) covers majority of debonded interface.

high-magnification optic microscope or electron microscope. When the sample was cut after being processed, the sample edge was polished. The polish powder filled the gap of the crack and we were unable to expel this filling material. However, Figure 9 provides some evidence which supports our claim that a debond exists. The edge photographs of the fibre in a single fibre composite sample, designed for transverse test, illustrate a clear circumferential interfacial debonding under the transversely applied stresses of 110 MPa (b) and 160 MPa (c). (a) is the comparison for the sample without any transverse loading. We know that there exists a compressive radial residual stress of approximately 380 MPa at the interface except the regions influenced by the free edge effect. The transversely applied stress will overcome the radial residual stress before it can create a positive interfacial radial stress to debond the interface. We define the radial stress concentration factor as the ratio of the radial stress around the circumferential fibre matrix interface in the interior of the composite to the applied stress. The maximum radial stress concentration factor, obtained using the approximate elasticity model, is 1.3. It means that the maximum radial stresses at the interface resulting from these applied stresses are far below the existing radial residual stress. Any interfacial debonding can only be the contribution of the free edge effect. Therefore, we believe that there exists an interfacial debond prior to any mechanical loading.

## CONCLUSIONS

A detailed study of the free edge effect on redistribution of residual stresses, radial residual stress reversal, and interfacial debonding has been carried out through theoretical modelling, numerical analysis, and experimental investigation. Although it has not been optically seen, a circumferential interfacial debond, approximately 20  $\mu\text{m}$  long starting at the free edge, is predicted to exist prior to any mechanical loading. Both the approximate elasticity model and the finite element model predicted (a) a radial residual stress reversal and a high tensile stress gradient at the fibre/matrix interface in the neighbourhood of free edge, and (b) a high gradient compressive stress at the corner of the fibre tip and a region of tensile radial stress in the matrix between the fibre tip and the free edge for the embedded fibre problem. The

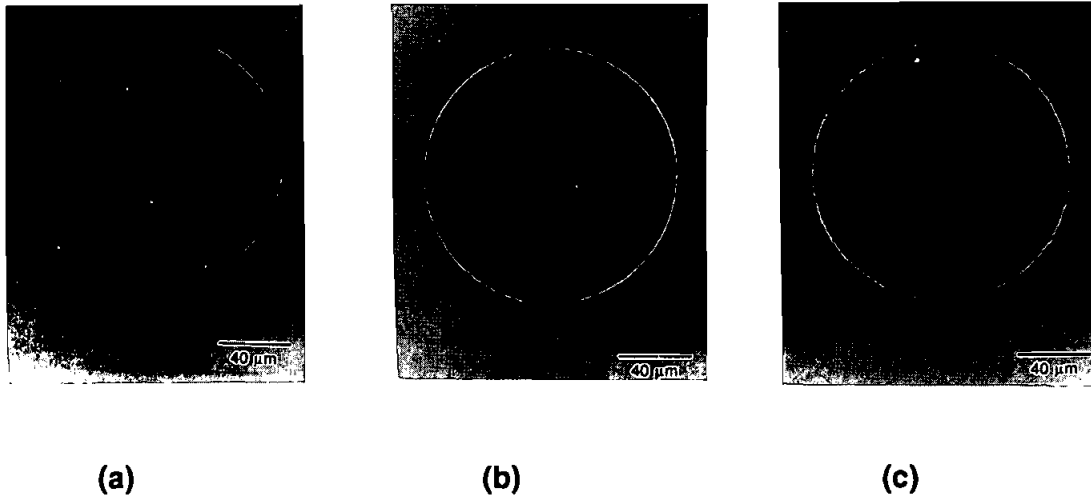


Figure 9. The edge photographs of the fibre in a single composite transverse test sample under (a) no applied stress, (b) a transversely applied stress of 110 MPa, and (c) a transversely applied stress of 160 MPa.

consistency between the approximate elasticity model and the finite element model indicates that both models, though approximate, are capable of analysing complex stress state at the interface of bi-material system. In addition, the results from both analytical and numerical analyses imply a radial stress singularity which is tensile for the free edge problem and compressive for the embedded fibre problem under thermoelastic cool down.

There are several reasons why it is difficult to quantitatively characterize the interfacial debond due to the edge effect. The first occurs, as explained earlier, after the edge of the sample being polished. This process fills the expected gap with polish powder which prevents us from seeing the gap using an optical or electron microscope. Also, the elastic constants of the 'debris' are unknown. We are not able to quantify the ultrasonic coefficient of reflection at the debonded area according to the equation expressed earlier. Next, although the presence of the debond is manifested in the ultrasonic image of the fibre, the ultrasonic C-scan system we were using has the finest step of 1 mil or  $25.4 \mu\text{m}$  which is larger than the debond and, therefore, is not able to measure accurately the interfacial debond. In addition, for a 25-MHz transducer the focal area diameter, which is approximately equivalent to the wavelength of the shear wave in the matrix materials, can be as large as  $150 \mu\text{m}$  in this case. Again this makes it only possible to detect the existence of the debond.

A higher-frequency transducer will result in a signal with a shorter wavelength, which will lead to a better resolution. For our single fibre composite sample the fibre is embedded about 1.1 mm under the sample top surface; i.e., the signal must travel 1.1 mm before it meets the fibre matrix interface. Despite the contribution of other effects, the signal attenuation is proportional to the frequency. If we used a transducer with a frequency higher than 25 MHz, the reflective signal would suffer a substantial attenuation which would eventually cause the experiment to fail. Even though at present we cannot quantitatively characterize the interfacial debond resulting from the free edge effect, the SBR technique together with the phenomenon of signal phase alteration allows us to indirectly detect an interfacial debond which is much smaller than the ultrasonic wave focal size. It provides a technique for detection of microscopic scale defects in composites using transducers with relatively low frequencies.

## ACKNOWLEDGEMENT

This work was supported by and performed on-site in the Materials Directorate, Air Force Wright Laboratory. Contact numbers are F33615-89-C-5612 (Karpur and Matikas) and F33615-90-C-5944 (Shaw). The first author, S. Hu, was sponsored by National Research Council–Wright Laboratory Program while this work was performed.

## REFERENCES

1. R.B. Pipes and N.J. Pagano, 'Interlaminar stresses in composite laminates under uniform axial extension', *J. Compos. Mater.*, **4**, 538 (1970).
2. N.J. Pagano, 'Axisymmetric micromechanical stress fields in composites', *Proc. 1992, IUTAM Symposium on Local Mechanics Concepts for Composite Material Systems*, Virginia Polytechnic Institute and State University, 1992, J.N. Reddy and K.L. Reifsnider (eds.), pp. 1–26. Springer-Verlag, Berlin.
3. N.J. Pagano, *Mechanics of Composite Materials—Selected Works of Nicholas J. Pagano*, edited by J. N. Reddy, Kluwer Academic Publishers, 1994.
4. E. Reissner, 'On a variational theorem in elasticity', *J. Math. Phys.*, **29**, 90–95 (1950).
5. G.P. Tandon, 'Use of concentric cylinder model as representative volume element for unidirectional fiber composites', *J. Comp. Mater.*, (1994) (in press).
6. R. C. Averill and G. P. Carman, 'Analytical modeling of micromechanical stress variations in continuous fiber-reinforced composites', *Proc. 1992, IUTAM symposium on Local Mechanics Concepts for Composite Material Systems*, Virginia Polytechnic Institute and State University, 1992, J. N. Reddy and K. L. Reifsnider (eds.), pp. 27–61. Springer-Verlag, Berlin.
7. R. Nimmer, R. J. Bankert, E. S. Russell, G. A. Smith, and P. K. Wright, 'Micromechanical modeling of fiber/matrix interface effects in transversely loaded SiC/Ti-6-4 metal matrix composites', *J. Comp. Tech. Res.*, **13**, 3–13 (1991).
8. X. J. Ning and P. Pirouz, 'The microstructure of SCS-6 SiC fiber', *J. Mater. Res.*, **6**, 2234–2248 (1991).
9. N. J. Pagano, unpublished work, 1994.
10. *ANSYS User's Manual for Revision 5.0*, Swanson Analysis Systems, Inc., 1992.
11. M. C. Waterbury, unpublished work, 1994.
12. T. E. Matikas and P. Karpur, 'Ultrasonic reflectivity technique for the characterization of fiber–matrix interface in metal matrix composites', *J. Appl. Phys.*, **74**, 228. (1993).
13. S. Hu, 'On the relation between composite free edge effect and ultrasonic image separation', unpublished work, 1994.
14. T. E. Matikas, P. Karpur, N. J. Pagano, S. Hu and L. L. Shaw, 'In-situ ultrasonic characterization of failure strength of fiber–matrix interface in metal matrix composites reinforced by SCS series fibers', *Review of Progress in Quantitative Nondestructive Evaluation*, **14B**, 1327–1332 (1994).
15. P. Karpur, T. E. Matikas and S. Krishnamurthy, 'Matrix–fibre interface characterization in metal matrix composites using ultrasonic imaging of fiber fragmentation', *Seventh Technical Conference on Composite Materials, Mechanics and Processing*, **1**, 420–427 (1992).
16. T. E. Matikas and P. Karpur, 'Micro-mechanics approach to characterize interfaces in metal and ceramic matrix composites', D. O. Thompson, D.E. Chimenti (eds.), *Review of Progress in Quantitative Nondestructive Evaluation*, **13B**, 1477–1484 (1993).
17. J. Krautkramer and H. Krautkramer, *Ultrasonic Testing of Materials*, 3rd edn, Springer-Verlag, New York, 1983.